ORIGINAL RESEARCH

20(S)-ginsenoside Rg3 promotes senescence and apoptosis in gallbladder cancer cells via the p53 pathway

Fei Zhang,* Maolan Li,* Xiangsong Wu,* Yunping Hu, Yang Cao, Xu'an Wang, Shanshan Xiang, Huaifeng Li, Lin Jiang, Zhujun Tan, Wei Lu, Hao Weng, Yijun Shu, Wei Gong, Xuefeng Wang, Yong Zhang, Weibin Shi, Ping Dong,# Jun Gu,# Yingbin Liu#

Department of General Surgery and Laboratory of General Surgery, Xinhua Hospital Affiliated to Shanghai Jiao Tong University, School of Medicine, Institute of Biliary Tract Disease, Shanghai Jiao Tong University School of Medicine, Shanghai, People's Republic of China

*These authors contributed equally to this work

#These authors jointly directed this work

Correspondence: Yingbin Liu; Ping Dong
Department of General Surgery and Laboratory of General Surgery, Xinhua Hospital Affiliated to Shanghai Jiao Tong University, School of Medicine, Institute of Biliary Tract Disease, Shanghai Jiao Tong University School of Medicine, Shanghai 200092, People's Republic of China
Email liuybphd@126.com; dongping1050@163.com

Abstract: Gallbladder cancer (GBC), the most frequent malignancy of the biliary tract, is associated with high mortality and extremely poor prognosis. 20(S)-ginsenoside Rg3 (20(S)-Rg3) is a steroidal saponin with high pharmacological activity. However, the anticancer effect of 20(S)-Rg3 in human GBC has not yet been determined. In this study, we primarily found that 20(S)-Rg3 exposure suppressed the survival of both NOZ and GBC-SD cell lines in a concentration-dependent manner. Moreover, induction of cellular senescence and G_0/G_1 arrest by 20(S)-Rg3 were accompanied by a large accumulation of p53 and p21 as a result of murine double minute 2 (MDM2) inhibition. 20(S)-Rg3 also caused a remarkable increase in apoptosis via the activation of the mitochondrial-mediated intrinsic caspase pathway. Furthermore, intraperitoneal injection of 20(S)-Rg3 (20 or 40 mg/kg) for 3 weeks markedly inhibited the growth of xenografts in nude mice. Our results demonstrated that 20(S)-Rg3 potently inhibited growth and survival of GBC cells both in vitro and in vivo. 20(S)-Rg3 attenuated GBC growth probably via activation of the p53 pathway, and subsequent induction of cellular senescence and mitochondrial-dependent apoptosis. Therefore, 20(S)-Rg3 may be a potential chemotherapeutic agent for GBC therapy.

Keywords: gallbladder cancer, 20(S)-ginsenoside Rg3, senescence, apoptosis, p53 pathway

Introduction

Gallbladder cancer (GBC) is the most common malignancy of the biliary tract, representing 80%–95% of biliary tract cancers worldwide, characterized by high lethality, late diagnosis and chemoresistance, it ranks sixth among gastrointestinal cancers.[1–3] Surgery is the only curative treatment for patients with GBC.[4] The majority of patients are diagnosed with advanced GBC, a stage at which treatment by resection is not possible.[5] Moreover, most patients have frequent recurrences following surgery and dismal outcomes after chemotherapy or radiotherapy.[6] The prognosis of patients with GBC in stage 0 and stage 1 is optimistic with 5-year survival rates ranging from 50% to 80%, but the prognosis in stage II–IV is dismal with 5-year survival rates ranging from 2% to 28%.[7] 5-Fluorouracil has been shown to have only a 20% response rate, and gemcitabine had a limited response rate of 36%.[8] Therefore, there is an urgent need to develop novel and effective therapy regimens for GBC patients.

Ginseng, such as American ginseng (*Panax quinquefolius* L.) and Asian ginseng (*Panax ginseng* CA Meyer), is the root of different *Panax* species (Araliaceae) and is one of the most commonly used traditional medicines.[9] Ginsenoside Rg3, one of the active ingredients in ginseng, has been reported to exhibit various

pharmacological and physiological effects.[10,11] Stereo-specific effects have been observed from this compound, with the 20(R) enantiomer, for instance, being more active as an antioxidant and in its promotion of the immune response,[12,13] and the 20(S) having a greater potential antidiabetic activity.[14] The 20(S) enantiomer is more suitable for pharmaceutical development because of its superior solubility compared with the 20(R) enantiomer. The 20(S)-ginsenoside Rg3 has also been shown to be remarkably nontoxic and is well-tolerated in mice, rats, and dogs.[15–17] Rg3 may increase the efficacy of cancer chemotherapy, possibly through inhibitory effects on NF-κB and AP-1 activity,[17] and downregulation of angiogenesis associated with VEGF expression.[18] Recently, 20(S)-Rg3 has been found to affect growth and survival in several human cancers, including colon cancer, leukemia, and ovarian cancer.[19–21] There is currently no published data showing the involvement of 20(S)-Rg3 in human GBC.

In the present study, we investigated the effect of the 20(S)-Rg3 on cell growth and survival in human GBC cell lines to evaluate its antitumor activity. Our data show that 20(S)-Rg3 is capable of inhibiting GBC cell growth via facilitating cellular senescence and apoptosis. Effect of 20(S)-Rg3 on GBC growth was confirmed in vivo using a mouse xenograft model. Our data therefore suggests that the inhibitory effect of 20(S)-Rg3 on growth is functionally related to its promotion effect on cell senescence and apoptosis and that 20(S)-Rg3 could serve as a novel strategy in treating GBC.

Materials and methods
Drugs and reagents
20(S)-ginsenoside Rg3 was obtained from the National Institute for the Control of Pharmaceutical and Biological Products (Beijing, People's Republic of China), and the purity was at least 95% as determined by HPLC (high performance liquid chromatography). 20(S)-Rg3 was dissolved in dimethyl sulfoxide (DMSO) in a 400 mM stock solution and stored at −20°C, and diluted with fresh complete medium immediately before use. An equal volume of DMSO (final concentration <0.1%) was added to the controls.

3-(4,5-dimethylthiazol-2-yl)-2,5-diphenyl-tetrazolium bromide (MTT), Hoechst 33342, Rhodamine 123, and Cyclo-heximide (CHX) were purchased from Sigma-Aldrich (St Louis, MO, USA). Annexin V/PI apoptosis kit was purchased from Invitrogen (Carlsbad, CA, USA). Primary antibodies

against Bad, Bax, Bcl-2, Bcl-XL, cleaved-caspase 3 (Asp175), murine double minute 2 (MDM2), and β-actin were purchased from Cell Signaling Technology (Beverly, MA, USA). p53, p16[INK4A], and pRB antibodies were obtained from Santa Cruz Biotechnology (Santa Cruz, CA, USA). p21[CIP1] antibody was obtained from BD Biosciences (San Diego, CA, USA). Cyclin A and Cyclin B1 antibodies were purchased from Epitomics (Burlingame, CA, USA). PCNA (proliferating cell nuclear antigen) antibody was obtained from Abcam (Cambridge, UK).

Cell culture
Human GBC cell lines NOZ, GBC-SD, SGC-996, EH-GB-1, and EH-GB-2 were purchased from the Cell Bank of Type Culture Collection of the Chinese Academy of Sciences (Shanghai, People's Republic of China). NOZ cells were maintained in William's medium (Gibco, Grand Island, NY, USA) supplemented with 100 U/mL penicillin–streptomycin (Hyclone, Logan, UT, USA) and 10% fetal bovine serum (FBS; Gibco). GBC-SD cells were maintained in DMEM (Dulbeccos' Modified Eagle's Medium) medium (Gibco) containing 10% FBS. These cell lines were cultured at 37°C in a humidified incubator containing 5% CO_2.

Cell viability assay
NOZ and GBC-SD cells were seeded into 96-well plates at a density of 5×10^3 cells per well, incubated overnight, and then treated with 20(S)-Rg3 at different concentrations (0, 25, 50, 100, 200, and 400 μM) for 24, 48, and 72 hours. In vitro cytotoxicity of the GBC cells was measured by using MTT assay, as previously described.[22]

Colony formation assay
NOZ and GBC-SD cells were seeded into 6-well plates at a density of 500 cells per well, and treated with different concentrations (0, 25, 50, 100, 200, and 400 μM) of 20(S)-Rg3 for 48 hours. After removal of the supernatant, the cells were allowed to form colonies in complete medium for 12 days. Next, cells were fixed with 4% paraformaldehyde and stained with 0.1% crystal violet (Sigma-Aldrich). After washing, the plates were air-dried, and stained colonies were photographed using a microscope (Leica, Wetzlar, Germany).

Senescence β-galactosidase assay
NOZ and GBC-SD cells were treated with different concentrations (0, 25, 50, 100, 200, and 400 μM) of

20(S)-Rg3 for 48 hours. Senescent cells were analyzed using a senescence-associated β-galactosidase (SA-β-gal) staining kit (Beyotime, Nantong, People's Republic of China) according to the manufacturer's instructions. The staining results were recorded as "positive" or "negative", according to a previous report.[23]

Cell cycle analysis

NOZ and GBC-SD cells were treated with different concentrations (0, 25, 50, 100, 200, and 400 μM) of 20(S)-Rg3 for 48 hours. The cells were harvested by trypsinization, washed twice in cold PBS (phosphate buffered saline), and fixed in 70% ethanol overnight at 4°C. Cell cycle was then detected by flow cytometry with PI (propidium iodide) staining according to a previous report.[24] At least 50,000 stained cells were analyzed on a FACS Caliber system for each determination.

Hoechst 33342 staining

Apoptotic cells were identified on the basis of morphological changes in their nuclear assembly by observing chromatin condensation and fragment staining with Hoechst 33342, as previously described.[24]

Annexin V/PI analysis

NOZ and GBC-SD cells were treated with different concentrations (0, 25, 50, 100, 200, and 400 μM) of 20(S)-Rg3 for 48 hours. Apoptosis was analyzed using an Annexin V/PI apoptosis kit according to the manufacturer's instructions, as previously described.[25]

Mitochondrial membrane potential (ΔΨm) assay

The ΔΨm was analyzed by fluorescence microscopy using the Rhodamine 123 probe.[26] After treatment with different concentrations of 20(S)-Rg3 for 48 hours, the supernatant was removed and the cells were washed with PBS twice and then stained in Rhodamine 123 staining solution (5 μg/mL) at 37°C for 30 minutes. The samples were analyzed by using a flow cytometer (BD Biosciences).

Western blot analysis

NOZ and GBC-SD cells were treated with different concentrations (0, 25, 50, 100, 200, and 400 μM) of 20(S)-Rg3 for 48 hours, and whole-cell lysates were prepared for Western blot analysis according to a previous report.[25]

Real-time polymerase chain reaction (PCR) analysis

Total RNA was extracted using Trizol reagent and reverse transcribed to cDNA by M-MLV reverse transcriptase according to the manufacturer's instructions. Specific cDNAs were then amplified by qPCR using the following primers: p53-forward, 5′-GAGGGATGTTTGGGAGATGTAA-3′; p53-reverse, 5′-CCCTGGTTAGTACGGTGAAGTG-3′; GAPDH-forward, 5′-TGCACCACCAACTGCTTAGC-3′; GAPDH-reverse, 5′-GGCATGGACTGTGGTCATGAG-3′. *GAPDH* gene was amplified as an internal control. qPCR products were detected with SYBR Green on BioRad Connet Real-Time PCR platform. Relative quantitation was analyzed by $2^{-\Delta\Delta CT}$ method.

In vivo efficacy of 20(S)-Rg3

Six-week-old BALB/c homozygous (nu/nu) nude mice (~18 g body weight) were purchased from Shanghai SLAC Laboratory Animal Co., Ltd. (Shanghai, People's Republic of China). All animal treatments were carried out in accordance with the National Institutes of Health Guide for the Care and Use of Laboratory Animals, and approved by the Institutional Animal Care and Use Committee of Shanghai Jiaotong University. The mice were maintained in a specific pathogen-free environment. After 1 week, NOZ cells (2×10^6) in 100 μL PBS were injected into the right flank of nude mice. After another week, these mice were randomly divided into five groups. Three groups (seven mice/group) received an intraperitoneal (IP) injection of PBS, 20 mg/kg of 20(S)-Rg3, and 40 mg/kg of 20(S)-Rg3 every day, respectively, and were sacrificed to detect tumor weight after 3 weeks. The other two groups (10 mice/group) was administered an IP injection of PBS and 20(S)-Rg3 at 40 mg/kg every day, respectively, for survival analysis. Immunohistochemical analysis was performed as described previously.[27]

Immunofluorescence staining

The expression of PCNA and cleaved caspase-3 was detected by immunofluorescence. Deparaffinized 4-μm tissue sections were cultured with PCNA or cleaved caspase-3 antibody. Subsequent antibody detection was carried out with Alexa Fluor 488 goat anti-mouse IgG secondary antibody. Sections were examined with a fluorescence microscope (Leica), and merged images were formed using Adobe Photoshop CS4.

Statistical analysis

All data are expressed as mean values ± standard errors from at least three independent experiments. Statistical

significance was calculated using the Student's *t*-test, and a *P*-value less than 0.05 was considered significant in all tests. All analyses were performed using the SPSS software version 19.0 (SPSS Inc, Chicago, IL, USA).

Results
20(S)-Rg3 decreases viability and proliferation of GBC cells in a dose-dependent manner

To evaluate the toxic effect of 20(S)-Rg3 on GBC, five human GBC cell lines were treated with 20(S)-Rg3 at different concentrations (0, 0.1, 1, 10, 100, and 1,000 μM) for 24 and 48 hours. MTT assay showed that 20(S)-Rg3 exhibited a concentration-dependent and time-dependent killing of diverse GBC cell lines, with an IC_{50} (half maximal inhibitory concentration) value of around 100 μM (Figure S1A and B). Therefore, GBC cells were treated with 20(S)-Rg3 in the range of the drug concentrations (25–400 μM) in vitro. GBC-SD cell line was more sensitive to 20(S)-Rg3 than other cell lines, while NOZ cell line was less sensitive compared to other cell lines (Figure 1A–D). Besides, the proliferative rate of GBC-SD cell line was much lower than other cell lines, while that of NOZ cell line was much higher (Figure S1C). Therefore, NOZ and GBC-SD cell lines were chosen as optimal cell models for subsequent functional analyses.

The ability of GBC cells to form colonies in the presence of 20(S)-Rg3 was assessed by colony formation assay (Figure 1E). 20(S)-Rg3 induced a dose-dependent decrease in both the number and the size of colonies formed in NOZ and GBC-SD cells (Figure 1F and G). The results indicate that 20(S)-Rg3 may have a long-term inhibitory effect on the proliferation of GBC cells.

20(S)-Rg3 accelerates senescence of GBC cells

Morphological changes of NOZ and GBC-SD cells could be seen in Figure 2A and B. Both cell lines became enlarged and flattened, had more cytoplasmic vacuoles in a concentration-dependent manner, representing a senescence-like state. SA-β-gal is of lysosomal origin and appears as the result of their increased biogenesis,[28] paralleled by increased expression of the *GLB1* gene encoding acidic lysosomal β-galactosidase,[29] making it a widely used marker of senescent cells in vitro and in vivo. As shown in Figure 2C and D, the higher the concentration of 20(S)-Rg3, the more SA-β-gal positive cells in both cell lines was observed. Moreover, the protein amounts of p53 and p21[Cip1] increased in senescent

cells but not the p16 and pRB protein (Figure 2E). These results suggest that the growth arrest in GBC cells results from an increase in p53-mediated p21 expression as cells enter senescence.

20(S)-Rg3 blocks cell cycle progression of GBC cells

Cellular senescence, which can be defined as a stress response preventing the propagation of cells that have accumulated potentially oncogenic alterations, is invariably associated with a permanent cell cycle arrest. To determine whether cell cycle arrest is responsible for 20(S)-Rg3-induced decrease in cell viability, flow cytometry was performed, which showed that the percentage of cells in G_0/G_1 phase was significantly increased in both cell lines following 20(S)-Rg3 treatment, while cell populations in S phase and G_2/M phase were simultaneously reduced (Figure 3A and B). These results indicate that 20(S)-Rg3 could arrest the cell cycle at G_0/G_1 phase in a dose-dependent manner. Western blot further confirmed that the levels of the S-related protein Cyclin A and the G_2/M-related protein Cyclin B1 were down-regulated in NOZ and GBC-SD cells following 20(S)-Rg3 treatment (Figure 3C).

20(S)-Rg3 triggers mitochondrial-related apoptosis of GBC cells

We could also see from flow cytometric DNA-histogram that cells were accumulated in the sub-G_1 phase following 20(S)-Rg3 treatment. Hoechst 33342 staining was thus performed to examine the nuclear morphology. In control cells, the nuclei were stained weakly, and homogeneously blue, whereas, in cells treated with 20(S)-Rg3 some bright chromatin condensation and nuclear fragmentation were observed (Figure 4A). The numbers of apoptotic nuclei containing condensed chromatin increased significantly as the 20(S)-Rg3 concentration increased (Figure 4B). PI staining also showed a dose-dependent increase in necrosis in both cell lines after 20(S)-Rg3 treatment (Figure S2). A marked dose-dependent increase in both the early and late stages of apoptosis was observed in NOZ and GBC-SC cells following 20(S)-Rg3 treatment by flow cytometry analysis with Annexin V-FITC [fluorescein isothiocyanate]/PI staining (Figure 4C and D). These results from different apoptosis assays reveal significant features of apoptosis, which strongly suggest that 20(S)-Rg3-mediated inhibition of cell growth in GBC is closely correlated with the enhanced apoptosis.

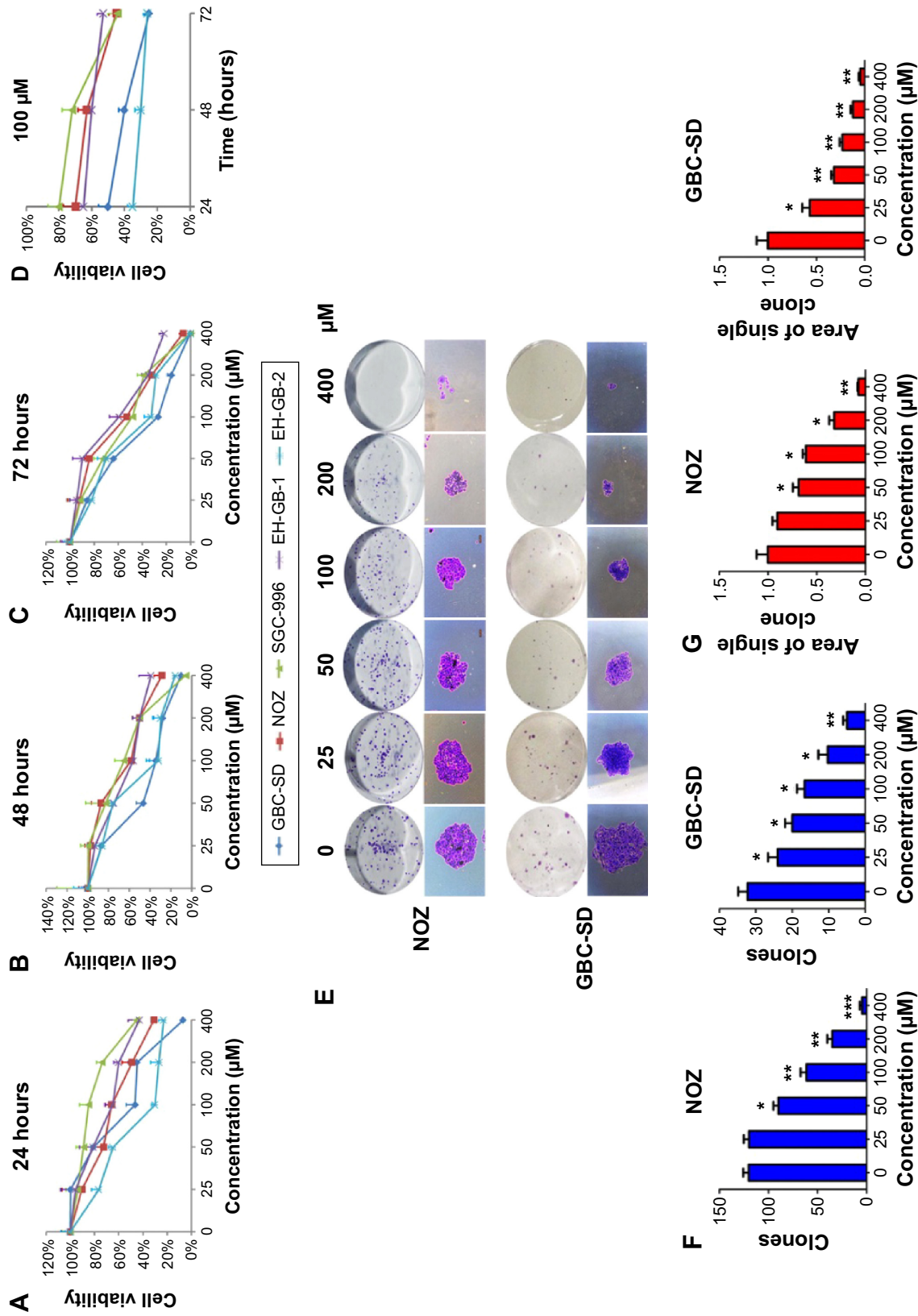To determine whether the cell apoptosis was dependent or independent of mitochondria, we tested whether

Figure 1 20(S)-Rg3 inhibits the viability and proliferation of GBC cells.
Notes: Cell viability was assessed using an MTT assay. (**A–C**) Five human GBC cell lines were treated with 20(S)-Rg3 at different concentrations (0, 25, 50, 100, 200, and 400 μM) for 24, 48, and 72 hours. (**D**) Five human GBC cell lines were treated with 100 μM 20(S)-Rg3 for 24, 48, and 72 hours. (**E**) Representative photographs of colony formation are shown. 20(S)-Rg3 caused a concentration-dependent decrease in both colony numbers (**F**) and colony size (**G**). Data represent the mean ± SD of three independent experiments. *$P<0.05$, **$P<0.01$, ***$P<0.001$ vs control.
Abbreviations: GBC, gallbladder cancer; SD, standard deviation; vs, versus; MTT, 3-(4,5-dimethylthiazol-2-yl)-2,5-diphenyl-tetrazolium bromide.
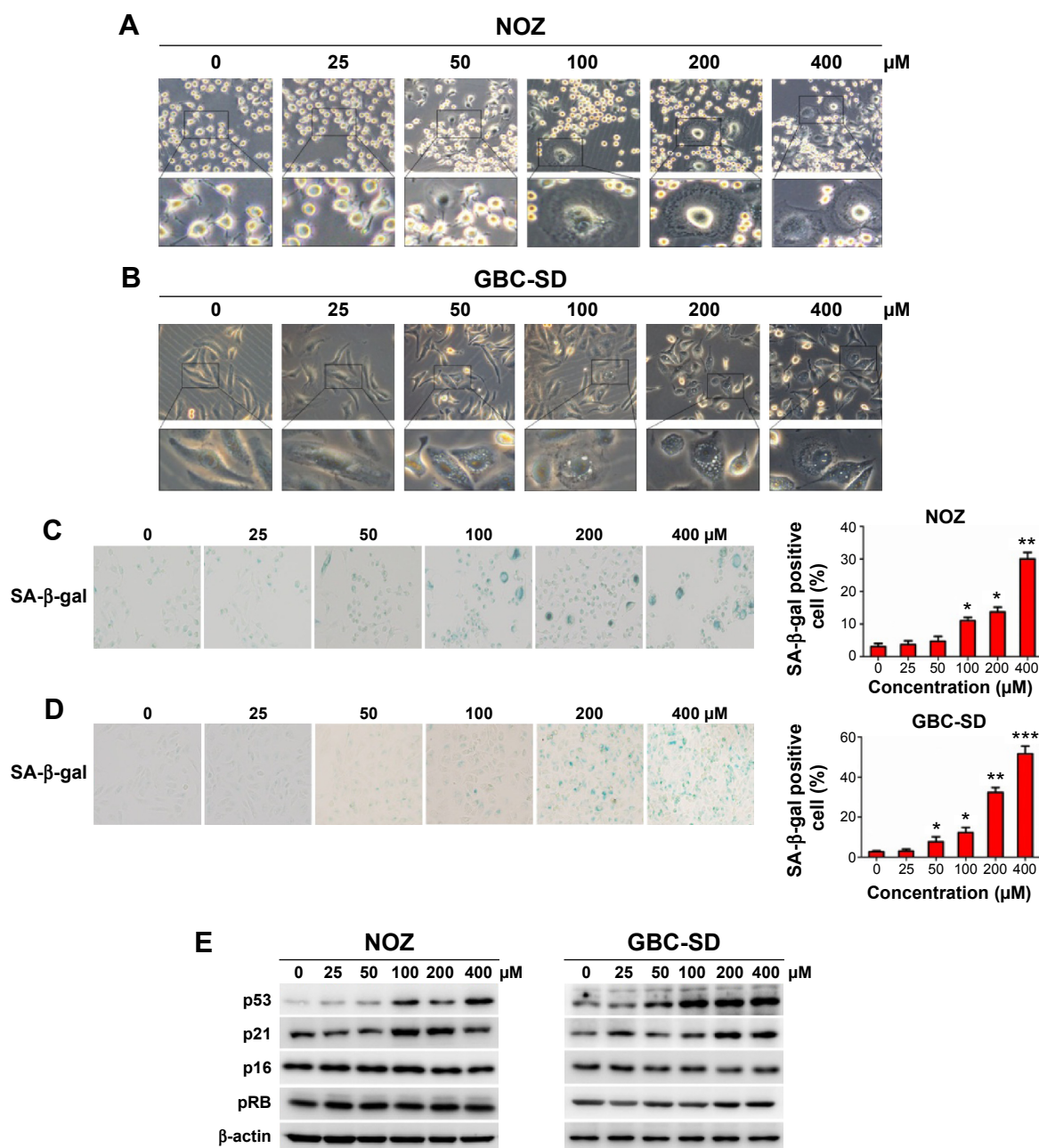
Figure 2 20(S)-Rg3 accelerates the senescence of GBC cells.
Notes: (**A**, **B**) Morphological changes of NOZ and GBC-SD cells were examined under a microscope. (**C**, **D**) Positive green-colored staining of senescent cells increased in both cell lines after 20(S)-Rg3 treatment. (**E**) Western blot analysis of senescence-related p53–p21 and p16–pRB pathways in both cell lines. β-actin was used as a loading control. Data represent the mean ± SD of three independent experiments. *$P<0.05$, **$P<0.01$, ***$P<0.001$ vs control.
Abbreviations: GBC, gallbladder cancer; SD, standard deviation; vs, versus.

20(S)-Rg3 caused a loss of mitochondrial membrane potential. Compared with control, 20(S)-Rg3 caused an obvious decrease of mitochondrial membrane potential in both NOZ and GBC-SD cells in a dose-dependent manner (Figure 4E and F).

Apoptosis is a type of programmed cell death that is caspase-dependent.[30] When NOZ and GBC-SD cells were treated with 20(S)-Rg3 at different concentrations, significant proteolytic cleavage of caspase-3 was detected using Western blot. The levels of pro- and antiapoptotic mitochondrial proteins Bad, Bax, Bcl-2, and Bcl-XL were also visualized by Western blot. 20(S)-Rg3 increased the expression of Bad and Bax, and conversely decreased Bcl-2 and Bcl-XL expression in both cell lines (Figure 4G). These results indicate that 20(S)-Rg3 could induce apoptosis in GBC cells through mitochondrial signaling pathways.
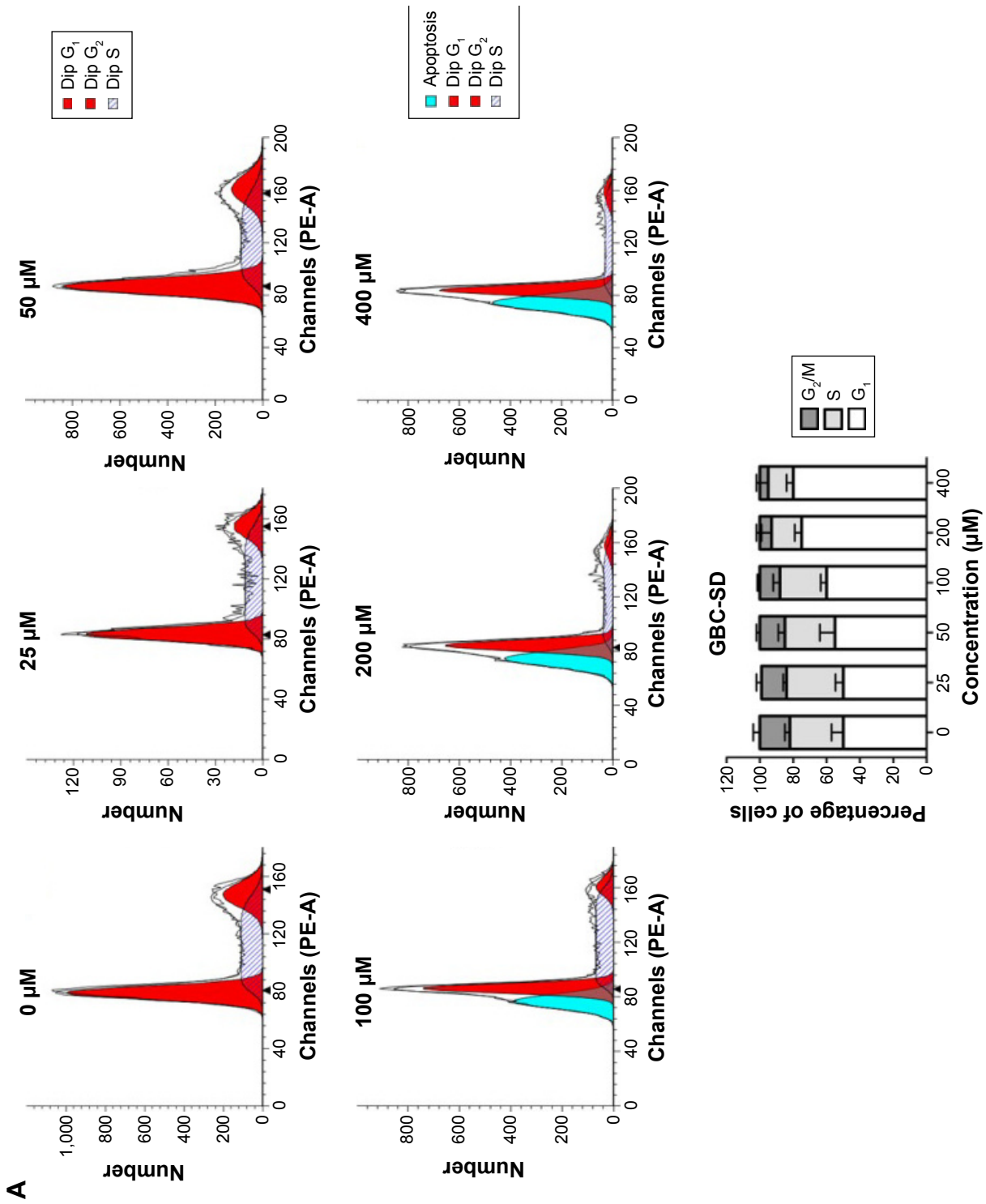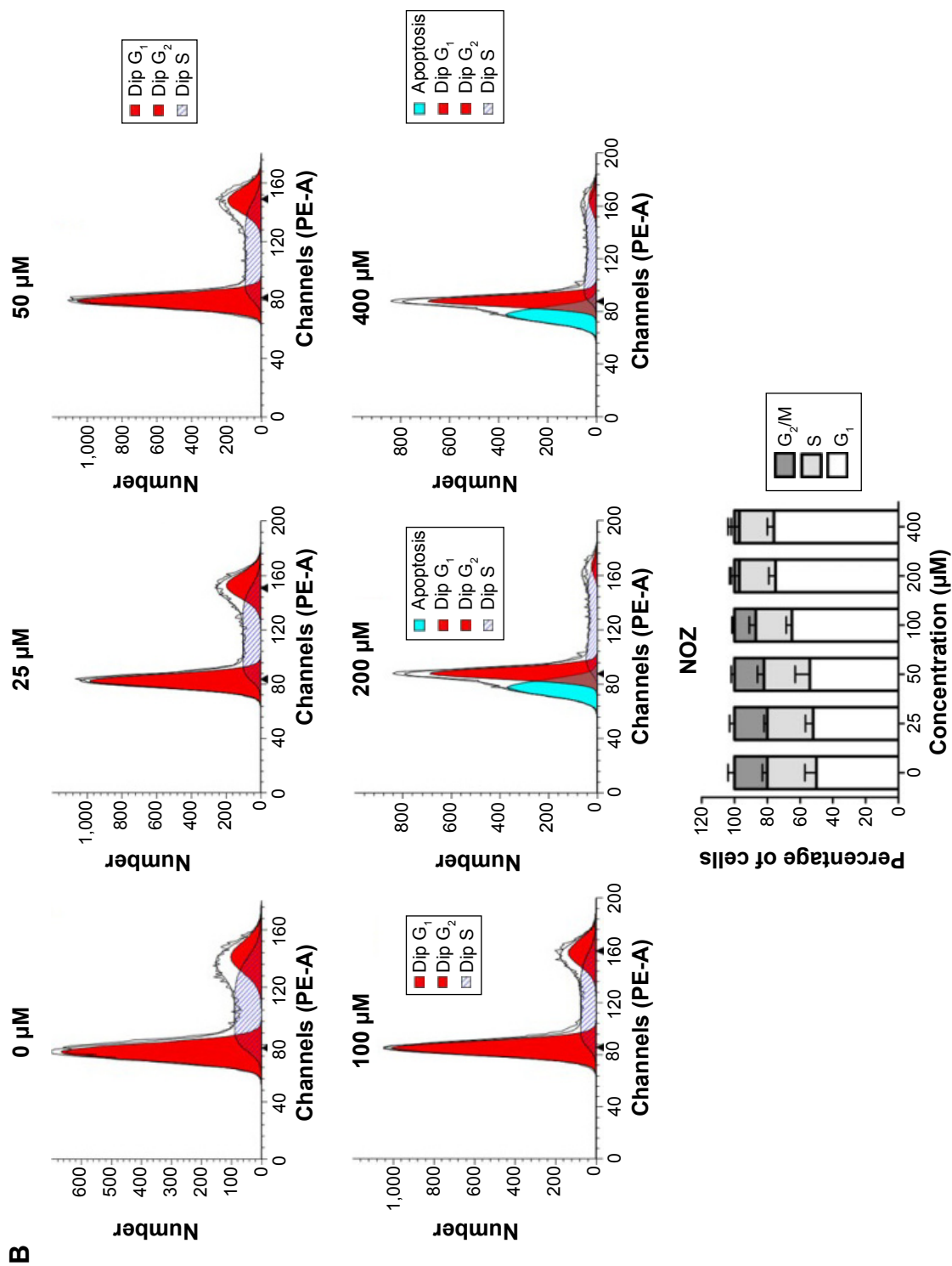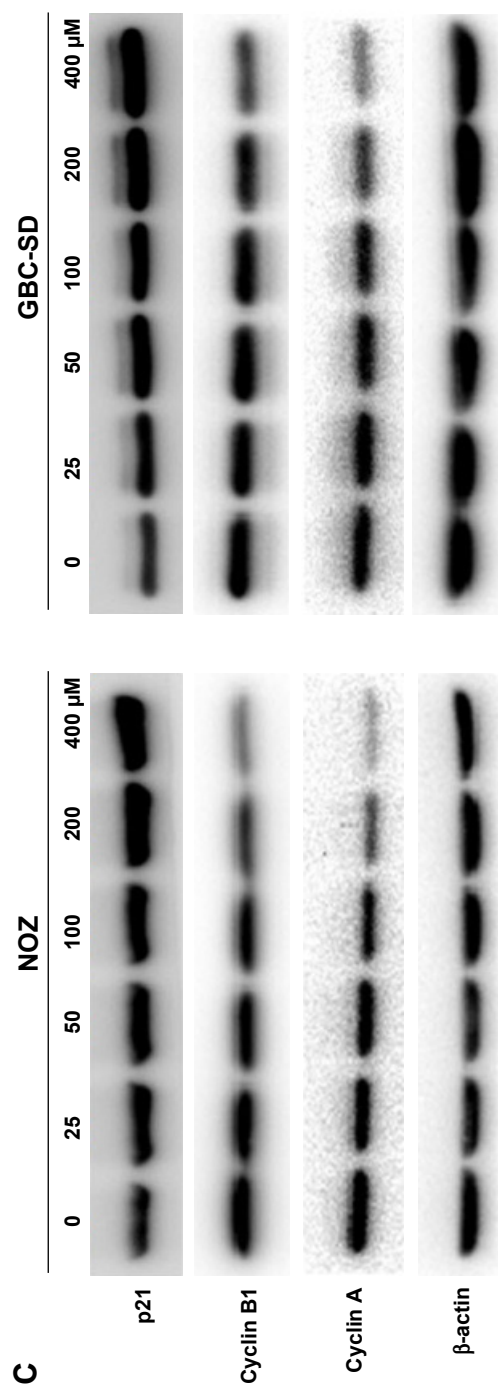
Figure 3 (*Continued*)

Figure 3 (*Continued*)

20(S)-Rg3 causes p53 accumulation via suppression of MDM2

p53 is a key player in tumor suppression, as it regulates cellular senescence, cell cycle arrest, and apoptosis. Thus, understanding the mechanism of p53 regulation is very important for cancer therapy.[31] Real-time PCR analysis revealed that 20(S)-Rg3 had no influence on the transcription level of p53 (Figure S3). We next investigated the involvement of the transcription-independent function of p53 using a protein synthesis inhibitor, (CHX), and found the suppressive effect of CHX on p53 protein accumulation was neutralized by 20(S)-Rg3 (Figure 5A and B). Western blot further showed that MDM2 protein levels were decreased by 20(S)-Rg3 treatment, in a dose- and time-dependent manner (Figure 5C and D). These results suggest that p53 protein levels were elevated as a result of MDM2 inhibition in GBC cells.

20(S)-Rg3 inhibits tumor growth in xenografted nude mice model by causing apoptotic cell death

To further evaluate whether 20(S)-Rg3 had an effect on inhibition of tumor growth in vivo, we measured the tumor volume in a xenograft tumor model in which NOZ cells were injected IP into nude mice. As shown in Figure 6A, we found that the drug concentration in the serum of mice with 40 mg/kg 20(S)-Rg3 administered IP daily for 1 week reached a peak at about 200 µM by a HPLC assay, which just fell within the range of the drug concentrations (25–400 µM) in vitro. So, 20 and 40 mg/kg of 20(S)-Rg3 were selected for in vivo experiments. When transplant tumors reached a mean group size of approximately 100 mm³, mice were treated every day for 3 weeks with various dose of 20(S)-Rg3. 20(S)-Rg3 showed a significant inhibitory effect on tumor volume and weight (Figure 6B–D). The survival of xenografted nude mice was prolonged after 40 mg/kg 20(S)-Rg3 treatment (Figure 6E). Moreover, SA-β-gal staining of tumor sections indicated that 20(S)-Rg3 caused tumor cell senescence. 20(S)-Rg3 dose-dependently induced a significant increase in p53 and p21[Waf1] expression (Figure 6F). In addition, tumor cell density and nuclear amount were both reduced. These results indicate that 20(S)-Rg3 inhibit tumor growth by causing cell senescence and apoptosis. Furthermore, PCNA expression was decreased, and caspase-3 activity was increased in 20(S)-Rg3 treatment groups (Figure 6G and H).

Discussion

Ginsenoside Rg3, which is the active component of ginseng, has various medical effects, such as antitumorigenic, anti-angiogenesic, and antifatiguing activities.[32] In particular, 20(S)-ginsenoside Rg3 may increase the antiproliferative effects of chemotherapy. In this study, we first identified the anticancer effect of 20(S)-Rg3 in human GBC.

20(S)-Rg3 exposure resulted in a dose- and time-dependent decrease in viability of all tested GBC cell lines. Moreover, vacuolization and SA-β-gal staining indicated
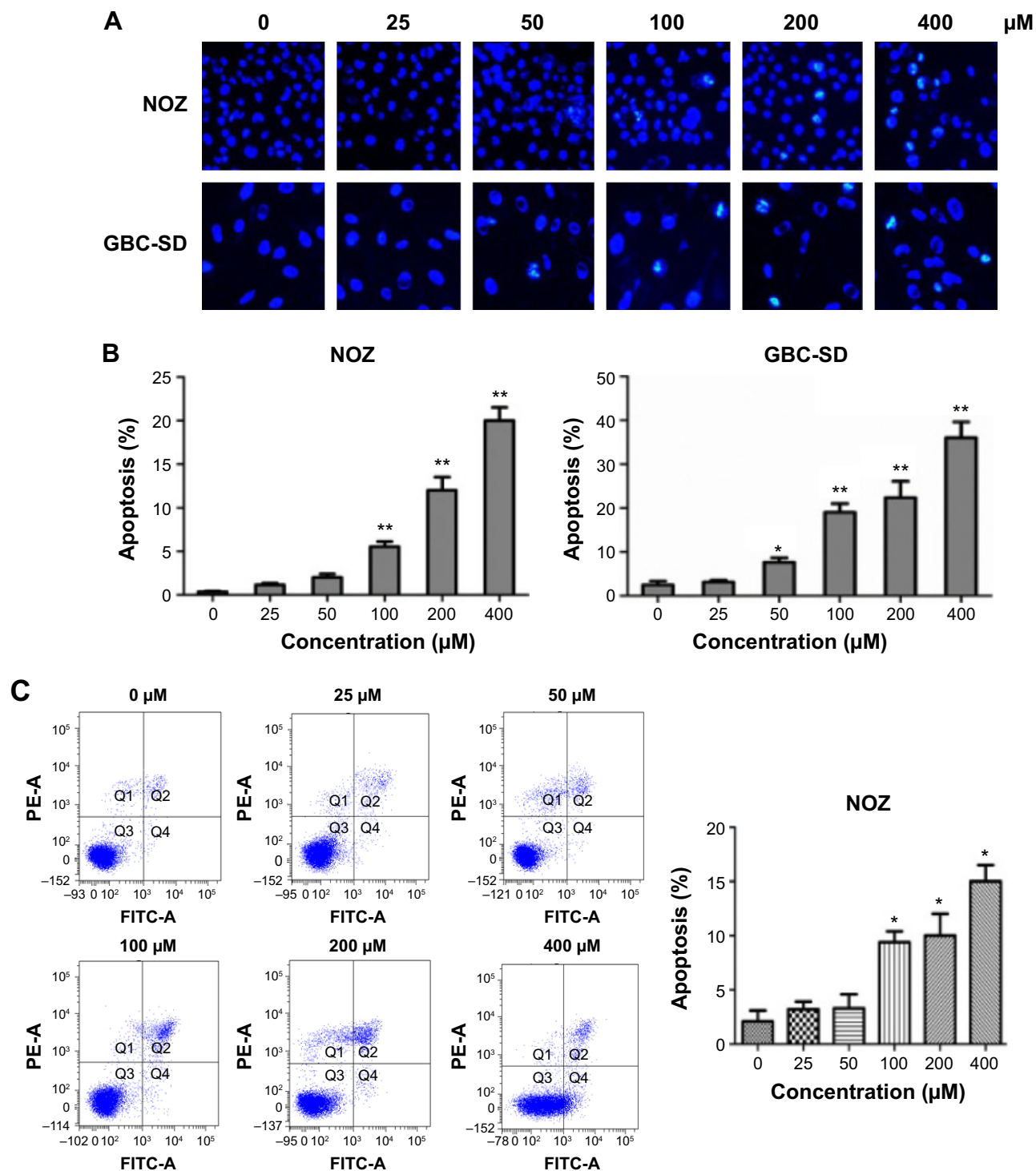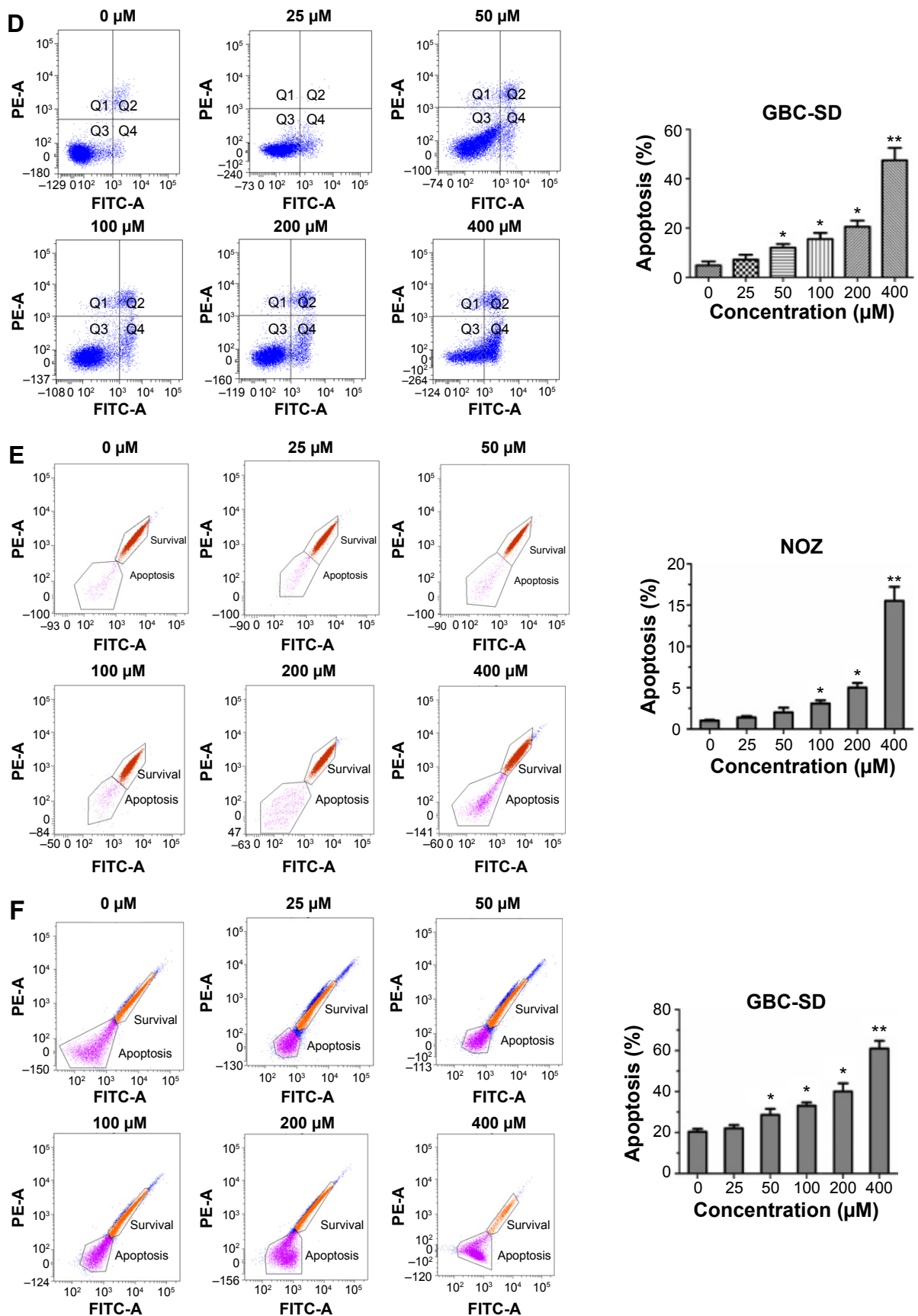
Figure 4 (*Continued*)

Figure 4 (*Continued*)

G
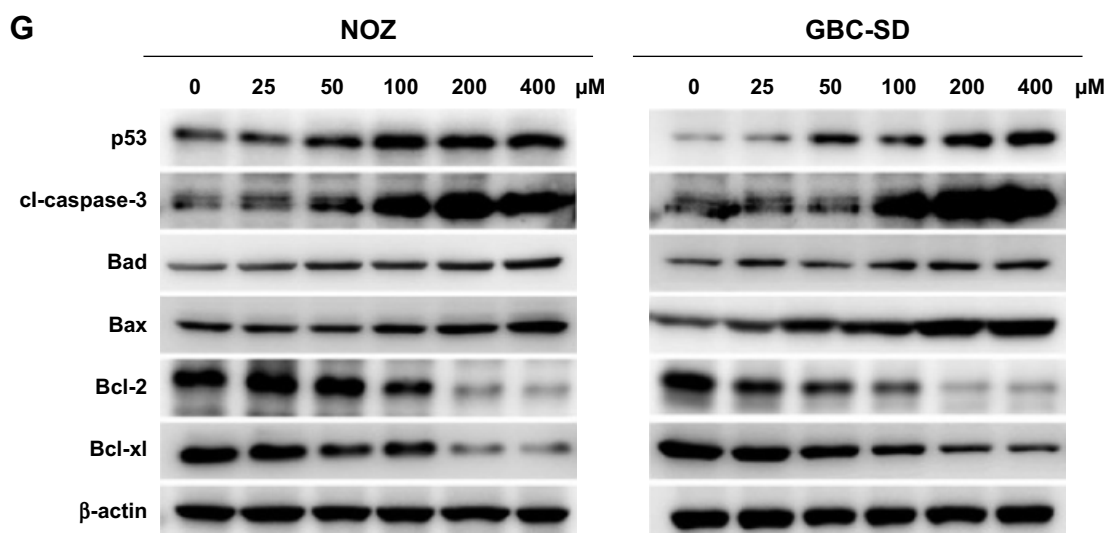
Figure 4 20(S)-Rg3 induces apoptosis in gallbladder cancer cells.
Notes: (**A**, **B**) Changes in apoptotic nuclear morphology were observed by Hoechst 33342 staining and visualized by fluorescent microscopy. (**C**, **D**) NOZ and GBC-SD cells were analyzed by flow cytometry with Annexin V-FITC/PI staining after 20(S)-Rg3 treatment. Annexin V vs PI plots from the gated cells showed the populations corresponding to viable (Annexin V–/PI–) and necrotic (Annexin V–/PI+), early (Annexin V+/PI–), and late (Annexin V+/PI+) apoptotic cells. (**E**, **F**) Flow cytometric analysis of ΔΨm. NOZ and GBC-SD cells were treated with 20(S)-Rg3 followed by Rhodamine 123 staining. Cells with high ΔΨm are marked "survival" and those with low ΔΨm are marked "apoptosis." Percentages of cells with low ΔΨm (apoptosis) are shown. (**G**) Western blot analysis of apoptosis-related proteins in both cell lines. β-actin was used as a loading control. Data represent the mean ± SD of three independent experiments. *$P<0.05$, **$P<0.01$ vs control.
Abbreviations: SD, standard deviation; FITC, fluorescein isothiocyanate; PI, propidium iodide; vs, versus.

that the impaired cell viability was probably partially dependent on the inducement of cellular senescence, which is an irreversible growth arrest characterized by decreased cell proliferation, combined with accumulation of mitotic defects and chromosomal instability,[33] representing an important tumor suppression mechanism. Classically, the p16/RB and p53/p21 axes are two major senescence-associated pathways in response to various stressors.[34] Increased p53 and p21[Cip1] expression were found in senescent cells induced by 20(S)-Rg3. p21 is a cell cycle inhibitor and tumor suppressor downstream of p53. A previous study reported that p53 and p21 act together to inactivate the Cyclin–Cdk complex in damaged cells, which could mediate G_0/G_1 and G_2/M arrest.[35] In this study, induction of G_0/G_1 arrest by 20(S)-Rg3 was accompanied by a large accumulation of p53 and p21.

It is well known that p53 can lead to induction of the apoptotic cascade.[36] To determine whether apoptotic cell death is responsible for the toxic effect of 20(S)-Rg3 on GBC cells, flow cytometry analysis with Annexin V/PI staining was performed and showed that apoptotic cells were significantly elevated following 20(S)-Rg3 treatment. The nuclear morphology observed by Hoechst 33342 staining also confirmed that 20(S)-Rg3 could cause apoptosis of GBC cells.

The related ginseng-derived 20(S)-ginsenoside Rh2 has been shown to induce apoptosis in leukemia Reh cells through mitochondrial signaling pathways.[37] As expected, 20(S)-Rg3

induced mitochondrial-related apoptosis through activation of caspase-3, upregulation of Bad and Bax expression, and downregulation of Bcl-2 and Bcl-XL expression in NOZ and GBC-SC cells. MDM2, a product of a p53-inducible gene, binds directly with the transactivation domain of p53 and assists in ubiquitin-proteasomal degradation of p53, thereby acting as a negative regulator.[38] 20(S)-Rg3 neutralized the ability of MDM2 to promote p53 degradation, leading to the stabilization and accumulation of p53. Previous studies have shown that 20(S)-Rg3 induces apoptosis in several human cancers. For instance, 20(S)-Rg3 promotes apoptosis in colon cancer cells through AMPK pathway.[19] 20(S)-Rg3-induced apoptosis in ovarian cancer cells is associated with PI3K/Akt and XIAP pathways.[21] Our data provide a novel mechanism for 20(S)-Rg3-induced apoptosis in GBC cells that involves the activation of p53 pathway through a mitochondria-dependent apoptotic cascade. Therefore, a model depicting our findings is presented in Figure 7. 20(S)-Rg3 down-regulates MDM2 expression in GBC cells, leading to the accumulation of p53. On one hand, p53-mediated p21 expression accelerates cellular senescence accompanied by a cell cycle arrest. On the other hand, the activation of p53 leads to induction of the mitochondria-dependent apoptotic cascade.

Furthermore, 20(S)-Rg3 potently inhibit tumor growth by inducing cell senescence and apoptosis in vivo. In addition, there was no significant difference in body weight
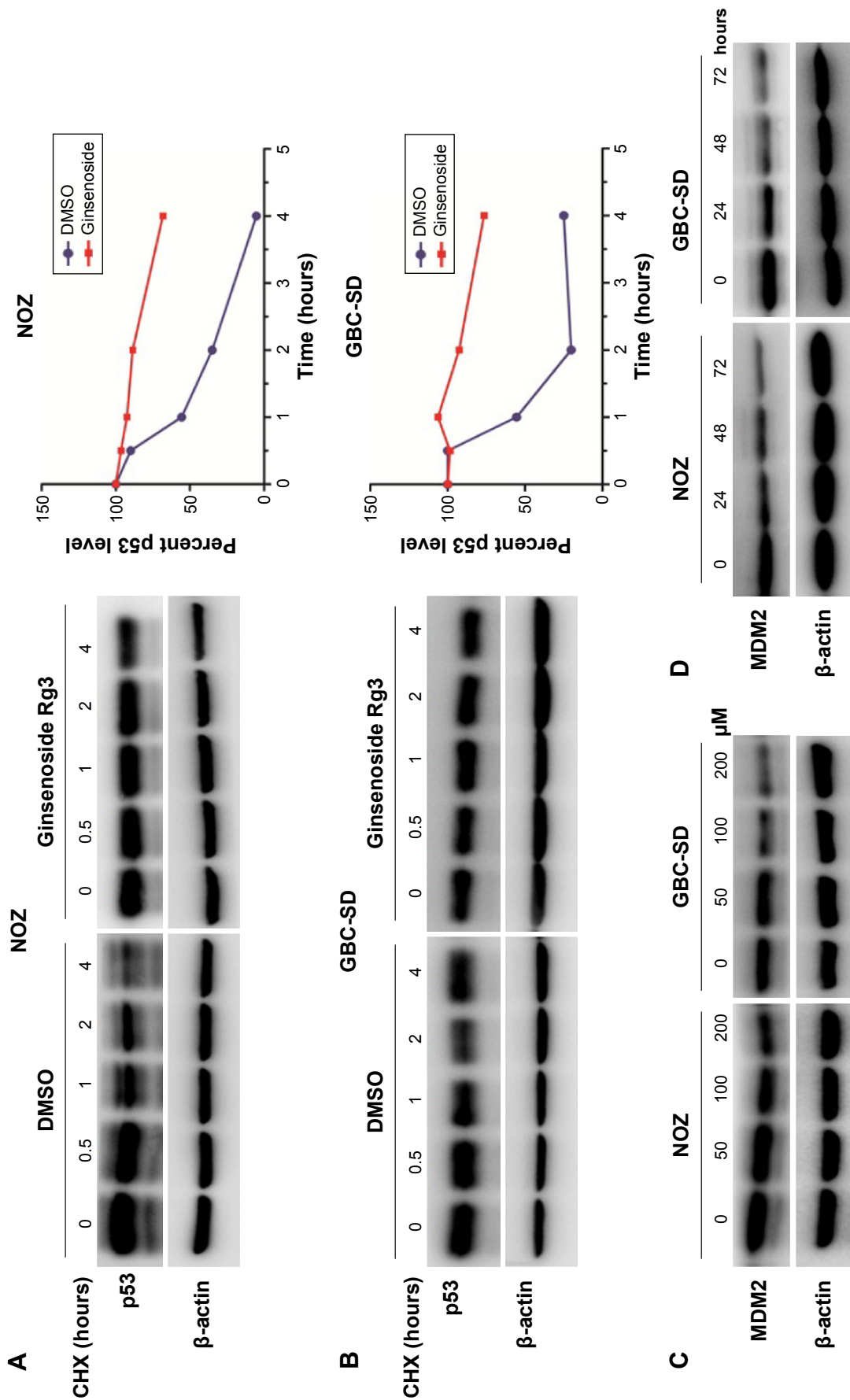
Figure 5 20(S)-Rg3 inhibits MDM2-mediated ubiquitination and degradation of p53.
Notes: (**A, B**) NOZ and GBC-SD cells were treated with CHX for 4 hours. Western blot analysis was carried out using an antibody specific for p53. β-actin was used as a loading control. (**C, D**) NOZ and GBC-SD cells showed a dose- and time-dependent decrease in MDM2 expression following 20(S)-Rg3 treatment. Data represent the mean ± SD of three independent experiments.
Abbreviations: CHX, cycloheximide; SD, standard deviation; DMSO, dimethyl sulfoxide.

(Figure 6A), blood routine, and hepatorenal function between the mice IP injected with 20(S)-Rg3 daily for 3 weeks and the mice treated with PBS (data not shown), suggesting 20(S)-Rg3 was not toxic for administration to mice in vivo and had potential clinical applications.

In conclusion, we suggest 20(S)-Rg3 as a potent growth inhibitor of GBC in vitro and in vivo. The mechanisms of 20(S)-Rg3 attenuating GBC growth may be via activation of the p53 pathway and subsequent induction of cellular senescence, which is a stress response that accompanies stable exit from the cell cycle, as well as activation of the mitochondrial-mediated intrinsic caspase pathway. Therefore, 20(S)-Rg3 has potential as a novel chemotherapeutic agent for GBC therapy.
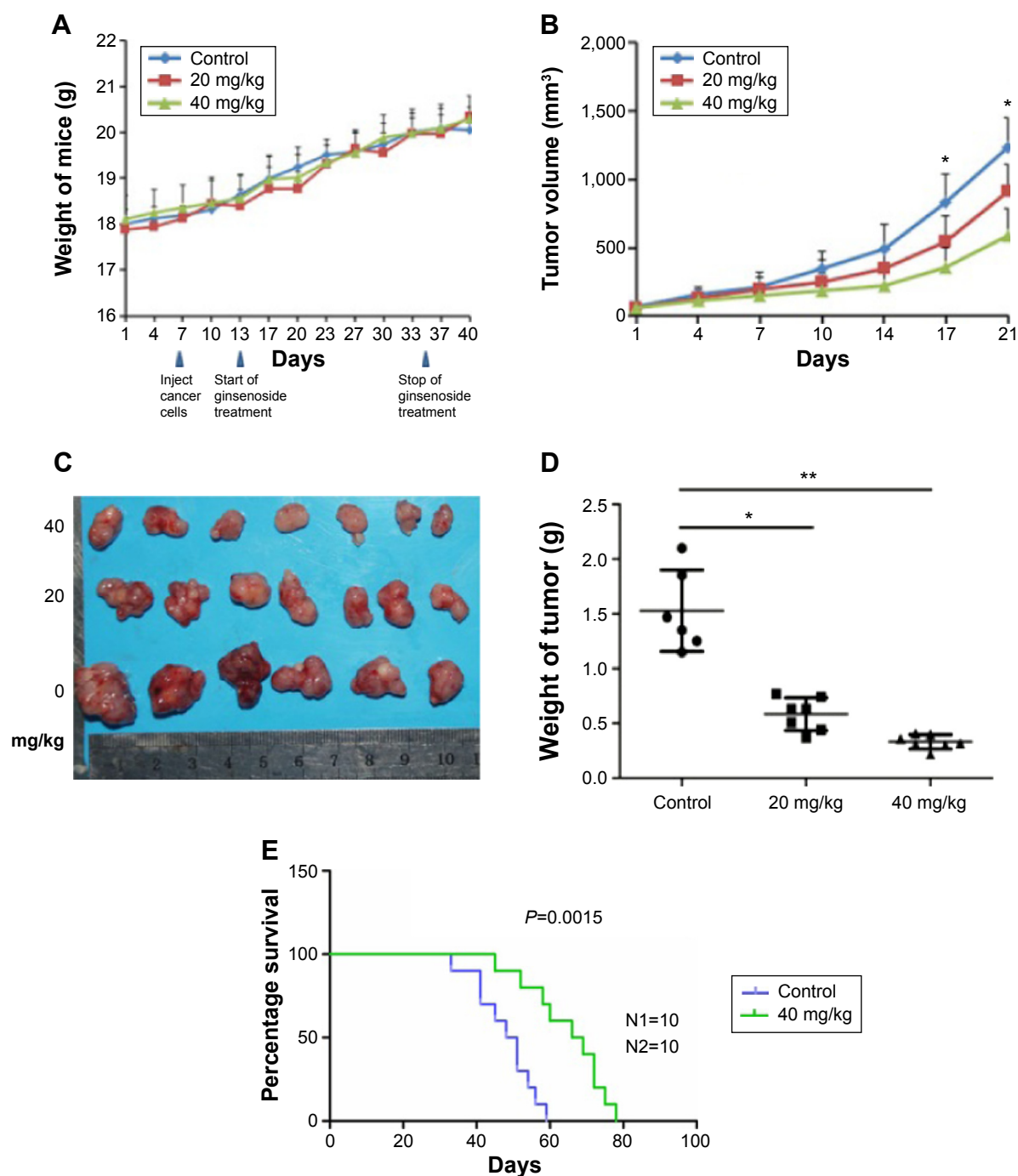
Figure 6 (Continued)
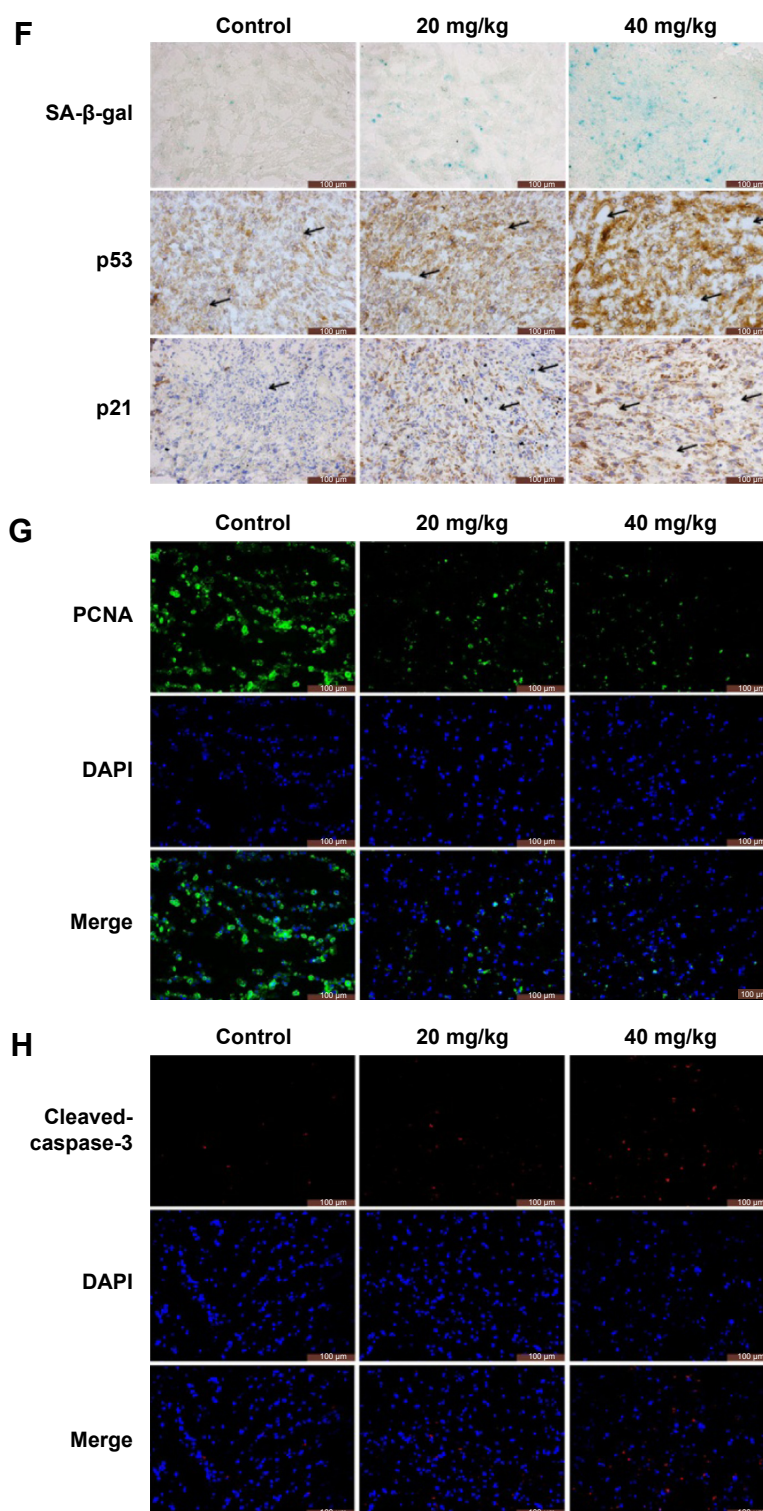
Figure 6 20(S)-Rg3 represses tumor growth in xenografted nude mice model by causing apoptotic cell death.
Notes: Tumor xenografts were established by subcutaneous inoculation of NOZ cells into the right flank of nude mice. (**A**) The mice were then administered 0.2 mL of vehicle (PBS) or 20(S)-Rg3 (20 and 40 mg/kg) IP every day for up to 3 weeks. (**B**) Tumor dimensions were periodically measured using calipers. (**C**, **D**) Photographs of representative tumors from each group are shown. Tumors were excised from the animals and weighed. (**E**) Survival curves of the mice in control and 20(S)-Rg3 (40 mg/kg) groups are shown. (**F**) SA-β-gal staining showed that 20(S)-Rg3 induced more senescent cells in tumor tissues. Vacuolization by 20(S)-Rg3 was accompanied by a large accumulation of p53 and p21 in tumor tissues. (**G**, **H**) Immunofluorescent images illustrate location of PCNA and cleaved-caspase-3 proteins in tumor tissues. Green fluorescence shows nuclear expression of PCNA, red fluorescence shows cytoplasmic expression of cleaved-caspase-3, and blue fluorescence shows all cell nuclei with patterns of DAPI staining. Data represent the mean ± SD of three independent experiments. *$P<0.05$, **$P<0.01$ vs control.
Abbreviations: DAPI, 4′,6-diamidino-2-phenylindole; PCNA, proliferating cell nuclear antigen; PBS, phosphate buffered saline; IP, intraperitoneal; SD, standard deviation; vs, versus; SA-β-gal, senescence-associated β-galactosidase.
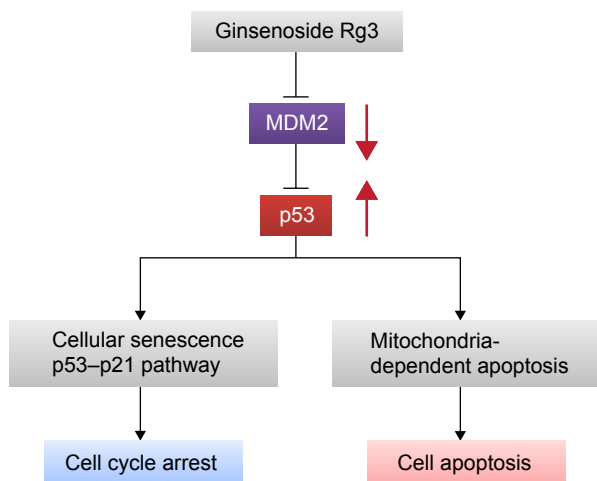
Figure 7 A working model for the action of 20(S)-Rg3 on gallbladder cancer cells.
Notes: 20(S)-Rg3 activates the p53 pathway, which induces both senescence and apoptosis in gallbladder cancer cells.

Disclosure

The authors report no conflicts of interest in this work.

References

1. Ma MZ, Li CX, Zhang Y, et al. Long non-coding RNA HOTAIR, a c-Myc activated driver of malignancy, negatively regulates miRNA-130a in gallbladder cancer. *Mol Cancer*. 2014;13:156.
2. Wang JW, Peng SY, Li JT, et al. Identification of metastasis-associated proteins involved in gallbladder carcinoma metastasis by proteomic analysis and functional exploration of chloride intracellular channel 1. *Cancer Lett*. 2009;281(1):71–81.
3. Li M, Zhang Z, Li X, et al. Whole-exome and targeted gene sequencing of gallbladder carcinoma identifies recurrent mutations in the ErbB pathway. *Nat Genet*. 2014;46(8):872–876.
4. Tan Z, Zhang S, Li M, et al. Regulation of cell proliferation and migration in gallbladder cancer by zinc finger X-chromosomal protein. *Gene*. 2013;528(2):261–266.
5. Hu YP, Tan ZJ, Wu XS, et al. Triptolide induces s phase arrest and apoptosis in gallbladder cancer cells. *Molecules*. 2014;19(2): 2612–2628.
6. Liu TY, Tan ZJ, Jiang L, et al. Curcumin induces apoptosis in gallbladder carcinoma cell line GBC-SD cells. *Cancer Cell Int*. 2013;13(1):64.
7. American Joint Committee on Cancer. Gallbladder. In: Edge S, Byrd DR, Compton CC, Fritz AG, Trotti FL, editors. *AJCC Cancer Staging Manual*. 7th ed. New York, NY: Springer; 2010:211–214.
8. Dutta U. Gallbladder cancer: can newer insights improve the outcome? *J Gastroenterol Hepatol*. 2012;27(4):642–653.
9. Poon PY, Kwok HH, Yue PY, et al. Cytoprotective effect of 20S-Rg3 on benzo[a]pyrene-induced DNA damage. *Drug Metab Dispos*. 2012;40(1): 120–129.
10. Jia L, Zhao Y. Current evaluation of the millennium phytomedicine – ginseng (I): etymology, pharmacognosy, phytochemistry, market and regulations. *Curr Med Chem*. 2009;16(19):2475–2484.
11. Jia L, Zhao Y, Liang XJ. Current evaluation of the millennium phytomedicine – ginseng (II): collected chemical entities, modern pharmacology, and clinical applications emanated from traditional Chinese medicine. *Curr Med Chem*. 2009;16(22):2924–2942.
12. Wei X, Su F, Su X, Hu T, Hu S. Stereospecific antioxidant effects of ginsenoside Rg3 on oxidative stress induced by cyclophosphamide in mice. *Fitoterapia*. 2012;83(4):636–642.
13. Wei X, Chen J, Su F, Su X, Hu T, Hu S. Stereospecificity of ginsenoside Rg3 in promotion of the immune response to ovalbumin in mice. *Int Immunol*. 2012;24(7):465–471.
14. Park MW, Ha J, Chung SH. 20(S)-ginsenoside Rg3 enhances glucose-stimulated insulin secretion and activates AMPK. *Biol Pharm Bull*. 2008;31(4):748–751.
15. Liu JP, Lu D, Nicholson RC, Li PY, Wang F. Toxicity of a novel anti-tumor agent 20(S)-ginsenoside Rg3: a 26-week intramuscular repeated administration study in Beagle dogs. *Food Chem Toxicol*. 2011;49(8): 1718–1727.
16. Liu JP, Lu D, Nicholson RC, Zhao WJ, Li PY, Wang F. Toxicity of a novel anti-tumor agent 20(S)-ginsenoside Rg3: a 26-week intramuscular repeated administration study in rats. *Food Chem Toxicol*. 2012;50(10): 3388–3396.
17. Lee JY, Jung KH, Morgan MJ, et al. Sensitization of TRAIL-induced cell death by 20(S)-ginsenoside Rg3 via CHOP-mediated DR5 upregulation in human hepatocellular carcinoma cells. *Mol Cancer Ther*. 2013;12(3): 274–285.
18. Kim DG, Jung KH, Lee DG, et al. 20(S)-Ginsenoside Rg3 is a novel inhibitor of autophagy and sensitizes hepatocellular carcinoma to doxorubicin. *Oncotarget*. 2014;5(12):4438–4451.
19. Yuan HD, Quan HY, Zhang Y, Kim SH, Chung SH. 20(S)-Ginsenoside Rg3-induced apoptosis in HT-29 colon cancer cells is associated with AMPK signaling pathway. *Mol Med Rep*. 2010;3(5):825–831.
20. Qiu XM, Bai X, Jiang HF, He P, Wang JH. 20-(s)-ginsenoside Rg3 induces apoptotic cell death in human leukemic U937 and HL-60 cells through PI3K/Akt pathways. *Anticancer Drugs*. 2014;25(9): 1072–1080.
21. Wang JH, Nao JF, Zhang M, He P. 20(s)-ginsenoside Rg3 promotes apoptosis in human ovarian cancer HO-8910 cells through PI3K/Akt and XIAP pathways. *Tumour Biol*. 2014;25(12):11985–11994.
22. Li S, Dong P, Wang J, et al. Icariin, a natural flavonol glycoside, induces apoptosis in human hepatoma SMMC-7721 cells via a ROS/JNK-dependent mitochondrial pathway. *Cancer Lett*. 2010;298(2): 222–230.
23. Te PR, Okorokov AL, Jardine L, Cummings J, Joel SP. DNA damage is able to induce senescence in tumor cells in vitro and in vivo. *Cancer Res*. 2002;62(6):1876–1883.
24. Bao R, Shu Y, Wu X, et al. Oridonin induces apoptosis and cell cycle arrest of gallbladder cancer cells via the mitochondrial pathway. *BMC Cancer*. 2014;14:217.
25. Wang XA, Xiang SS, Li HF, et al. Cordycepin induces S phase arrest and apoptosis in human gallbladder cancer cells. *Molecules*. 2014;19(8): 11350–11365.
26. Saris NE, Teplova VV, Odinokova IV, Azarashvily TS. Interference of calmidazolium with measurement of mitochondrial membrane potential using the tetraphenylphosphonium electrode or the fluorescent probe rhodamine 123. *Anal Biochem*. 2004;328(2):109–112.
27. Hui K, Yang Y, Shi K, et al. The p38 MAPK-regulated PKD1/CREB/Bcl-2 pathway contributes to selenite-induced colorectal cancer cell apoptosis in vitro and in vivo. *Cancer Lett*. 2014;354(1):189–199.
28. Kurz DJ, Decary S, Hong Y, Erusalimsky JD. Senescence-associated (beta)-galactosidase reflects an increase in lysosomal mass during replicative ageing of human endothelial cells. *J Cell Sci*. 2000;113(Pt 20): 3613–3622.

29. Lee BY, Han JA, Im JS, et al. Senescence-associated β-galactosidase is lysosomal β-galactosidase. *Aging Cell*. 2006;5(2):187–195.

30. Salvesen GS, Dixit VM. Caspases: intracellular signaling by proteolysis. *Cell*. 1997;91(4):443–446.

31. Rivlin N, Brosh R, Oren M, Rotter V. Mutations in the p53 tumor suppressor gene: important milestones at the various steps of tumorigenesis. *Genes Cancer*. 2011;2(4):466–474.

32. Kim YJ, Choi WI, Jeon BN, et al. Stereospecific effects of ginsenoside 20-Rg3 inhibits TGF-β1-induced epithelial-mesenchymal transition and suppresses lung cancer migration, invasion and anoikis resistance. *Toxicology*. 2014;322:23–33.

33. Ly DH, Lockhart DJ, Lerner RA, Schultz PG. Mitotic misregulation and human aging. *Science*. 2000;287(5462):2486–2492.

34. Salama R, Sadaie M, Hoare M, Narita M. Cellular senescence and its effector programs. *Genes Dev*. 2014;28(2):99–114.

35. Vogelstein B, Lane D, Levine AJ. Surfing the p53 network. *Nature*. 2000; 408(6810):307–310.

36. Schumacher M, Kelkel M, Dicato M, Diederich M. Gold from the sea: marine compounds as inhibitors of the hallmarks of cancer. *Biotechnol Adv*. 2011;29(5):531–547.

37. Xia T, Wang JC, Xu W, et al. 20S-Ginsenoside Rh2 induces apoptosis in human Leukaemia Reh cells through mitochondrial signaling pathways. *Biol Pharm Bull*. 2014;37(2):248–254.

38. Poyurovsky MV, Katz C, Laptenko O, et al. The C terminus of p53 binds the N-terminal domain of MDM2. *Nat Struct Mol Biol*. 2010; 17(8):982–989.
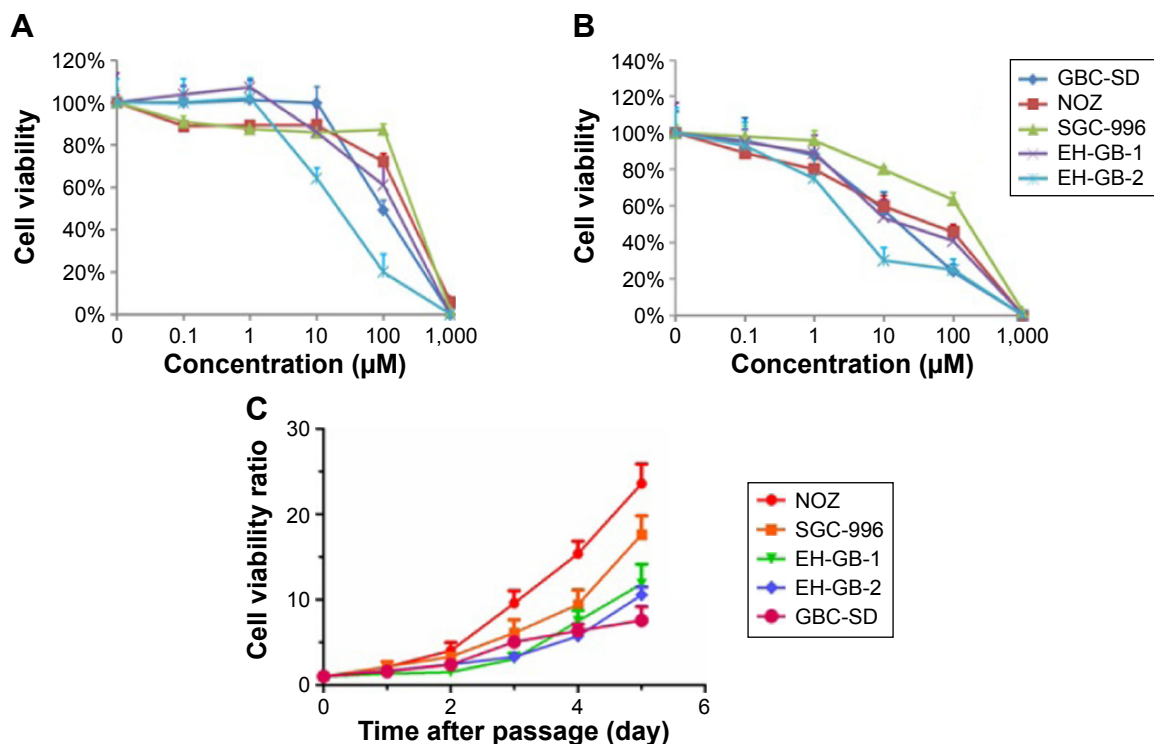
Supplementary materials

Figure S1 20(S)-Rg3 inhibits the viability of GBC cells.
Notes: (**A**, **B**) Five human GBC cell lines were treated with 20(S)-Rg3 at different concentrations (0, 0.1, 1, 10, 100, and 1,000 µM) for 24 and 48 hours. (**C**) Cell viability of these five GBC cell lines was assessed using an MTT assay.
Abbreviations: GBC, gallbladder cancer; SD, standard deviation; MTT, 3-(4,5-dimethylthiazol-2-yl)-2,5-diphenyl-tetrazolium bromide.
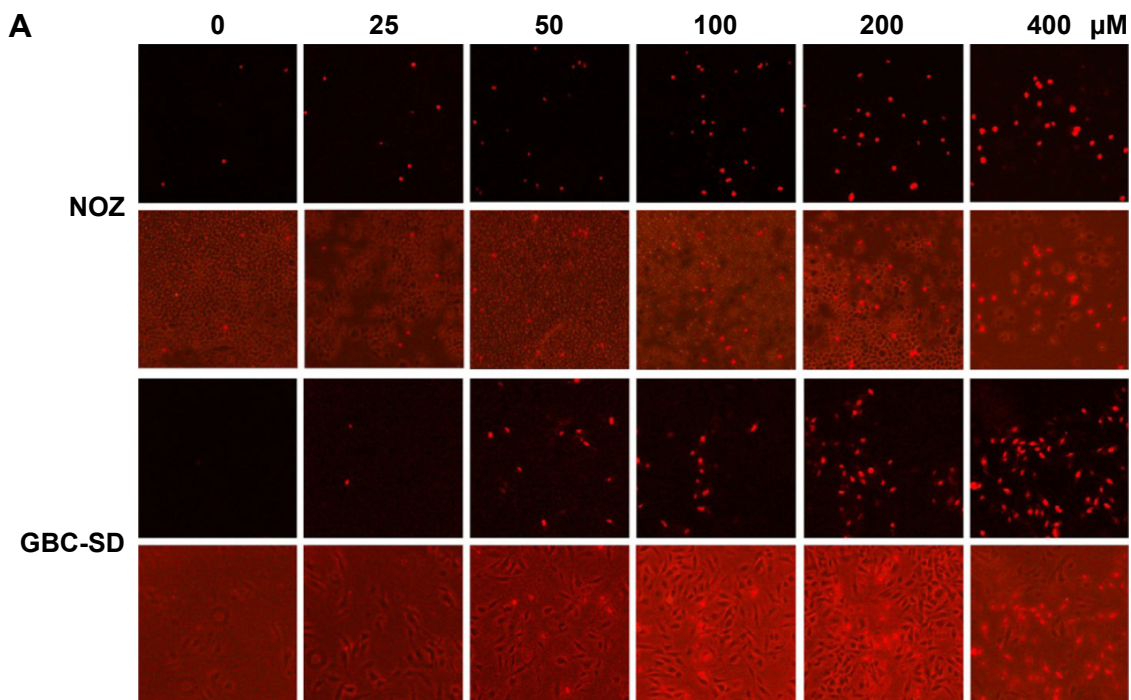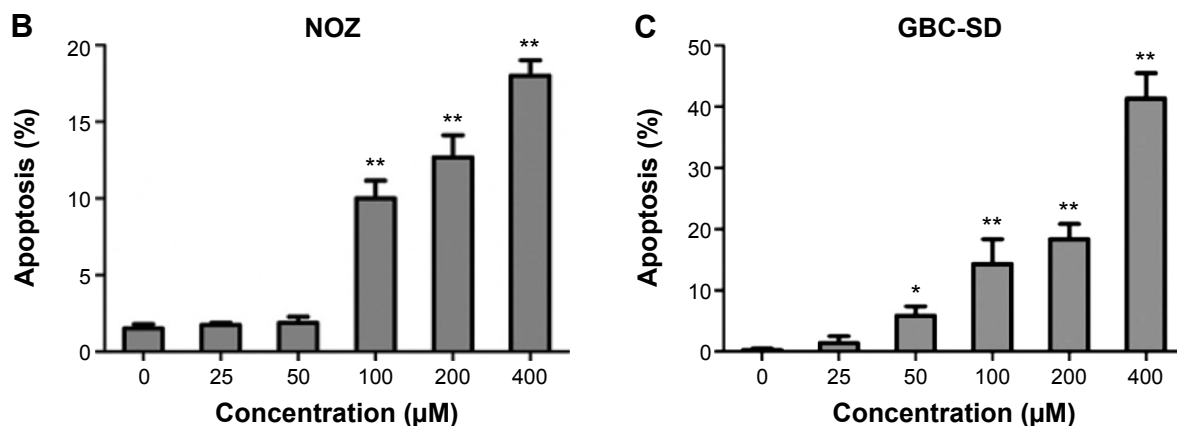

Figure S2 (*Continued*)

Figure S2 20(S)-Rg3 induces more necrotic cells in gallbladder cancer cells.
Notes: (**A**) PI staining showed a dose-dependent increase in necrosis in NOZ and GBC-SD cells treated with 20(S)-Rg3. (**B, C**) The percentage of apoptotic cells are shown by the histogram.
Abbreviations: PI, propidium iodide; GBC, gall bladder cancer; SD, standard deviation.
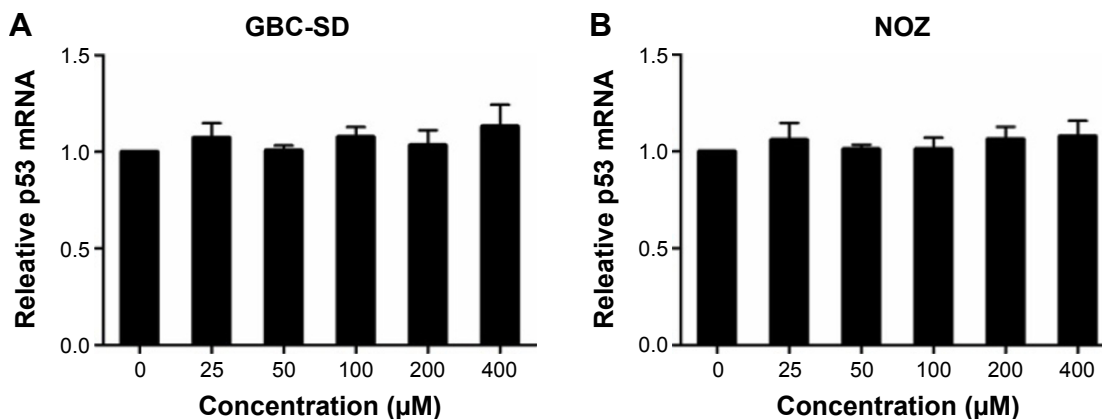

Figure S3 Real-time analysis of p53 mRNA levels in NOZ and GBC-SD cells after 20(S)-Rg3 treatment (**A**, **B**).
Note: *GAPDH* gene was amplified as an internal control.
Abbreviations: GBC, gall bladder cancer; SD, standard deviation.